- Determination of the effects of meteorology including moisture from the Gulf of Mexico on visibility-reducing particles.
- Evaluate and improve the accuracy of atmospheric models and source attribution methods through the use of atmospheric tracers and updated source emissions profiles.

2 Background

Visual air quality at a site depends largely upon the size, chemical composition, and concentration of atmospheric particles (aerosols). These aersosol properties are in turn dependent upon many factors, including: the relationship between the receptor site (e.g. Big Bend) and sources of pollutant emissions and the atmospheric transport and dispersion relating the source and receptor location, chemical transformation of emissions between source and receptor, (e.g. gas-to-particle conversion) wet or dry deposition, and relative humidity at the receptor.

Following a brief description of the Big Bend area will be a look at pollutant emissions for sulfur dioxide. The seasonally varying transport patterns affecting Big Bend National Park will then be examined, followed by a summary of light extinction and aerosol chemical component data for Big Bend. Finally, conditional probability plots will be shown indicating the probability that light extinction or chemical species were high at Big Bend when air passed over each geographic area en route to Big Bend.

2.1 Setting

In a remote area of southwestern Texas, where the Rio Grande makes a large U-turn along the US-Mexico border, lies an area known as the "Big Bend Country." Within this expanse lies BBNP, Texas,--a 324,247 hectare (1,252 square miles) reserve--established as a national park in 1944 and designated as a Biosphere Reserve in 1976. (Figure 2-1). Big Bend is a land of contrasts: the Rio Grande--portions of which have been designated as a Wild and Scenic River; desert--BBNP is 97 percent Chihuahuan Desert; and mountains--the Chisos Mountains--which tower 2400 meters (7800 feet) above the desert sea and the Sierra del Carmen across the river in Mexico. Along the Rio Grande are deep cut canyons--Santa Elena, Mariscal, and Boquillas--alternating with narrow valleys walled by towering cliffs (US Dept. of Interior, 1983). It is a region of large biological diversity containing more than 1,000 species of plants, including 65 cacti, 434 birds, 78 mammals, 71 reptiles and amphibians, and 35 fish (Big Bend Natural History Assoc., 1990). Endangered species include the peregrine falcon, black-capped vireo, Mexican long-nose bat, Big Bend gambusia (a fish), and three threatened cacti (Big Bend Natural History Assoc., 1990). Because of its contrasting landscapes, however, Big Bend is also known and appreciated for the beauty of its scenic vistas located in both countries.

Although early travelers called the land "*el despoblado*", the unpopulated land, there is a rich history associated with the land extending back in time to ca. 8500-6500

B.C. The Indians, the Spanish, the Mexicans and the Anglos have all been part of Big Bend's history (Big Bend Natural History Assoc., 1989). Nonetheless, the area is remote and sparsely populated, with approximately 13,000 people occupying an area about the size of the State of Maryland (12,407 square miles). In the 1930s many people who loved the Big Bend country saw that this land of contrast, beauty, and solitude was worth preserving for future generations--an effort that resulted in the establishment of Big Bend State Park and BBNP.

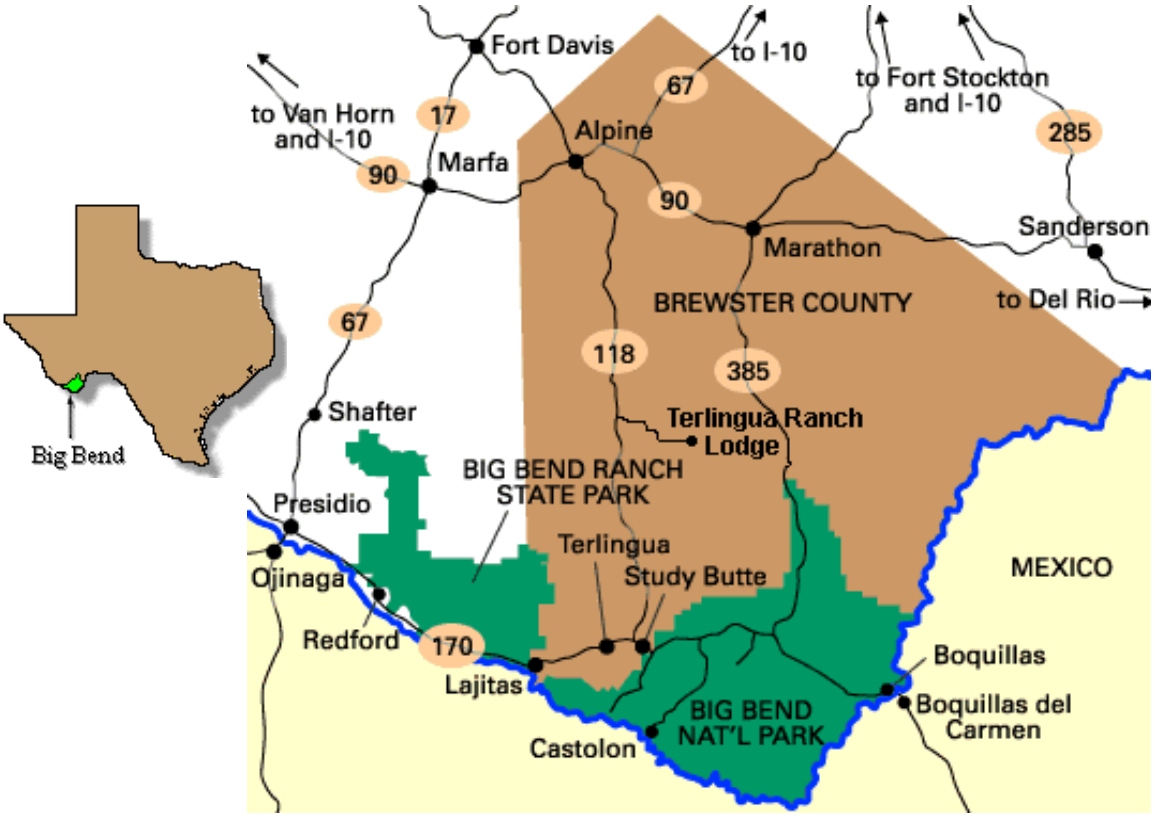

Figure 2-1. Location map of Big Bend National Park in southwestern Texas.

2.2 SO_2 Emissions Sources

According to the preliminary study and long-term monitoring at Big Bend, sulfate is an important component of haze at Big Bend National Park and results from atmospheric conversion of SO_2. Thus, emissions of SO_2 are of particular concern to the BRAVO study. Figure 1 is a map of the region that shows BBNP and the locations of SO_2 source areas of importance in Mexico and in Texas (other states in the region have much lower SO_2 emissions).

Major SO_2 sources in Texas include oil refineries, coal fired power plants, and carbon black producers. The majority of the Texas refineries are located along the eastern shore of Texas on the Gulf of Mexico. Historically, coal fired power plants were built along the lignite belt which runs from the northeast corner of Texas southwest

toward the Carbon I/II facilities in Mexico. Carbon black manufacturers are distributed along the east coast of Texas and near the oil fields in the Texas panhandle.

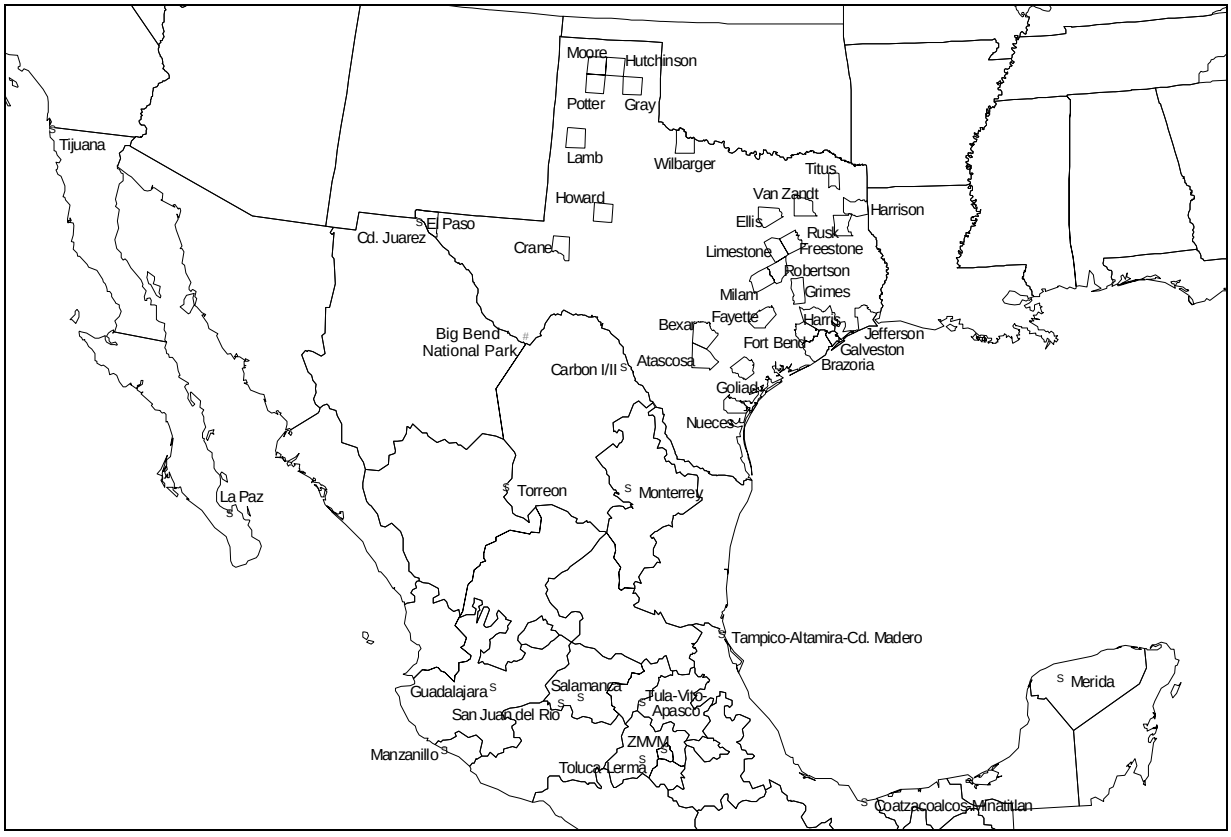

Figure 2-2: Site map of Mexican cities and Texas counties with SO_2 emissions greater than 5000 tons SO_2/yr. The location of Big Bend National Park is also shown.

Major SO_2 sources in Texas include oil refineries, coal fired power plants, and carbon black producers. The majority of the Texas refineries are located along the eastern shore of Texas on the Gulf of Mexico. Historically, coal fired power plants were built along the lignite belt which runs from the northeast corner of Texas southwest toward the Carbon I/II facilities in Mexico. Carbon black manufacturers are distributed along the east coast of Texas and near the oil fields in the Texas panhandle.

Major SO_2 emissions in Mexico are due largely to fuel oil refining and combustion and coal combustion. The Carbon I/II power plants are the largest coal combustion facilities in Mexico. Major refineries and industrial centers are located in Tampico on the east coast, Manzanillo on the west coast, Tula-Vito-Apasco north of Mexico City, and Toluca-Lerma south of Mexico City.

Figure 2-3 shows point source SO_2 emissions by 1 degree longitude by 1 degree latitude grid cells. The data is based upon information from Instituto Nacional de Ecologia (base year 1994) for Mexican cities with emissions greater than 5000 tons/year and the USEPA AIRS database. Figure 2 shows the greatest concentration of SO_2

emissions in the Ohio River Valley, although the numbers may not fully reflect recent reductions in SO_2 emissions in that area. Closer to Big Bend are significant sources in northern and central Mexico and eastern Texas.

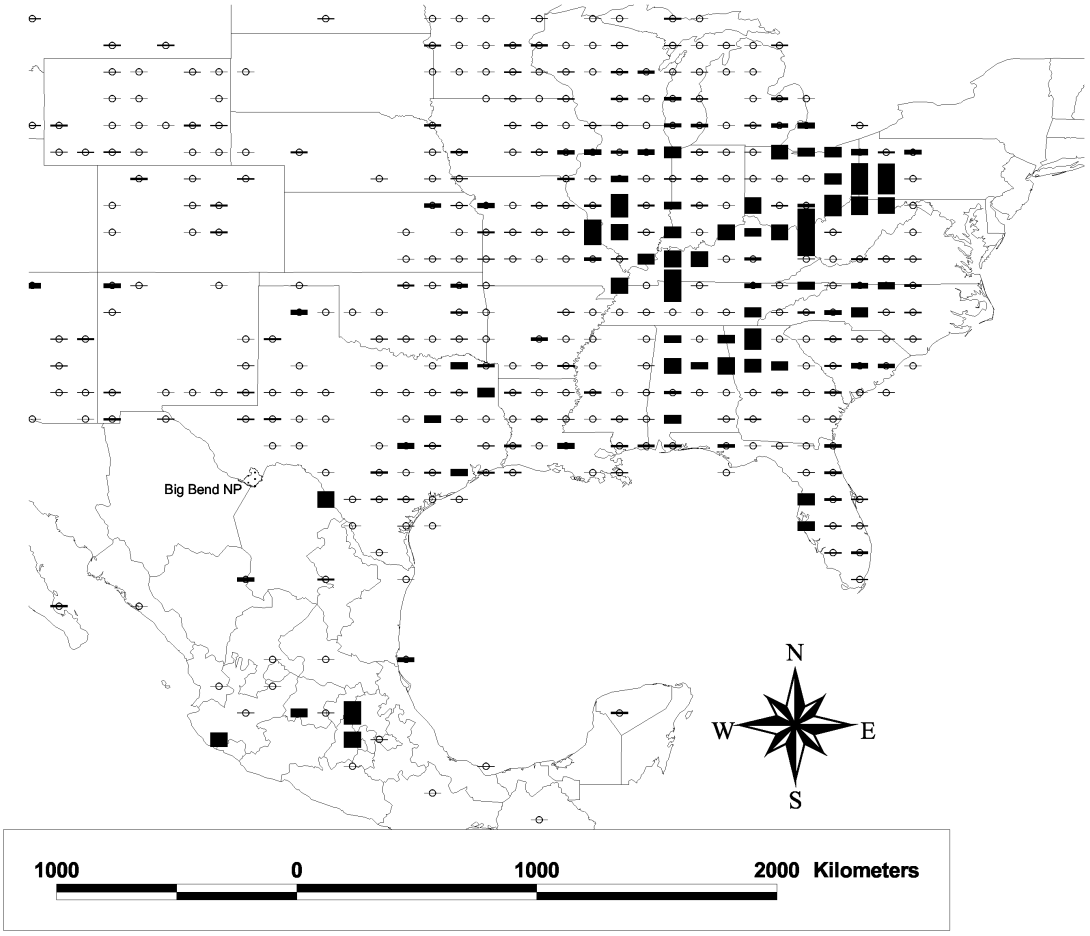

Figure 2-3. Point sources of SO_2 by 1 degree longitude by 1 degree latitude grid cells. The bar at Carbon I/II (see Figure 1) corresponds to 240,000 tons per year.

2.3 Transport Patterns

Transport patterns described here are based upon results of the Atmospheric Transport and Dispersion model (ATAD)(Heffter, 1980). The ATAD model has been used by many researchers for computing forward and backward air trajectories (e.g. Pitchford *et. al.*, 1981, White *et. al.*, 1994, Kahl *et. al.*, 1997, Green and Gebhart, 1997). Advantages of the model are that a long-period of record of upper air observations is available, and because the model requires little computational time, a large number of trajectories can be run for statistical analyses. Disadvantages include the observed winds are available for a somewhat sparse network, are typically collected only twice per day, a single layer-averaged wind is used, vertical motions are not considered, and the model is no longer supported so recent years cannot easily be run.

The ATAD model computes trajectories by averaging observed winds in space and time. It first computes a transport layer depth from temperature soundings using specified criteria to determine whether a significant inversion exists. It averages the winds within the transport layer at each site, then computes a distance weighted average of nearby sites to obtain a wind vector at the specified starting location. After computing the new trajectory position from the wind vector, the model repeats the entire process. For time steps between the observations (typically 12 hours apart), the model performs a temporal interpolation of observed winds as well as spatial interpolation. While individual trajectories may have substantial error, particularly after a few days of simulated transport, in the absence of systematic biases statistical properties based upon large numbers of trajectories should be valid.

Analysis involved using ATAD backtrajectories for Big Bend National Park for the period 1982-1994. A series of analyses were run that provided the frequency with which ATAD backtrajectories passed over 1 degree latitude by 1 degree longitude (1 x 1) grid cells. Frequencies were calculated for annual and one-half month periods to determine the seasonal variations in transport paths. Using light extinction and aerosol data at Big Bend, the probability of high light extinction and high chemical components of haze was determined for periods when backtrajectories went through each 1 x 1 grid cell. This type of analysis, in conjunction with emission density maps can give an *idea* of the regions and sources that are contributing to haze at Big Bend.

Figure 2-4 shows the percent of all ATAD backtrajectories from Big Bend for 1982-1994 that passed through each 1 x 1 grid cell. The total number of backtrajectories was 18,264. Because a 1 x 1 grid cell subtends a smaller angle as distance increases from Big Bend and the backtrajectories have no dispersion, cells at greater distances from Big Bend tend to have lower percentages of backtrajectories passing through them than cells nearer to Big Bend. However, the relative frequency of flows from different directions can be noted by considering the shape of the contoured frequency plot. In addition the tabulation of frequencies by 1 x 1 cells has the feature of weighting cells inversely by their distance from Big Bend, which may be appropriate when considering the effects of the dispersion of distant sources (neglecting conversion processes). In this and following figures, a small black circle (dot) is placed at the center of each grid cell with 10 or more backtrajectories passing through the cell. Contours (color shaded) should be ignored in areas with no dots.

From Figure 2-4, we see that the most frequent annual flow direction for Big Bend is from the southeast. However, substantial variations in average frequency of flow directions occur during the year. In late January, backtrajectories from the west and northwest are at their annual peak, while few backtrajectories come from cells far to the south of Big Bend (Figure 2-5). From late February through late April bimodal distribution is seen with flows mainly from the west and the southeast (e.g. see Figure 2-6), with the westerly mode shifting from west-northwest to west-southwest from February to April. From May through July, the flow becomes progressively more southeast and nearly all backtrajectories are from the southeast in July (Figure 2-7).

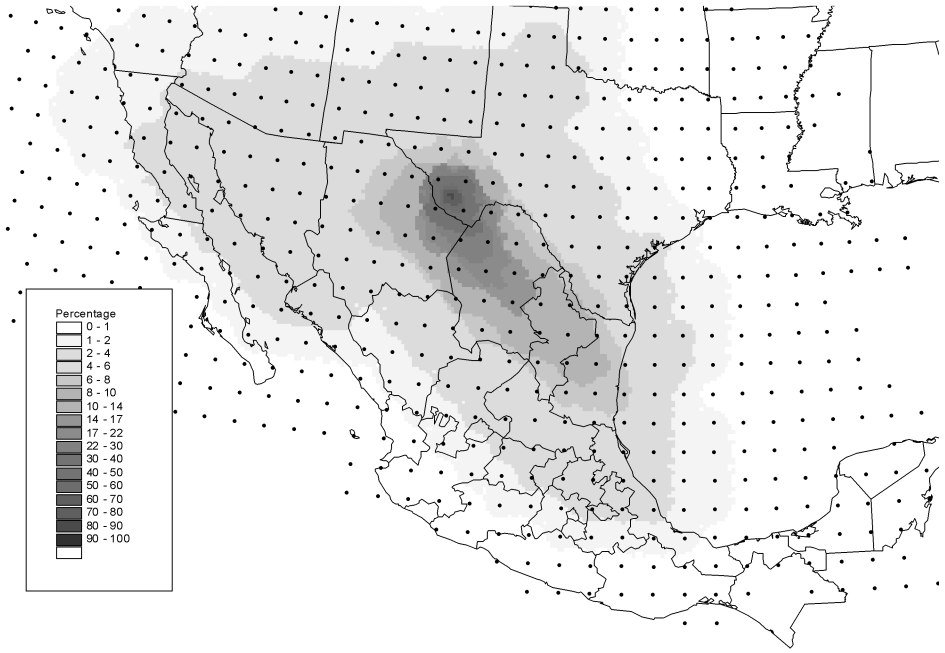

Figure 2-4 Annual trajectory frequency passing over cell.

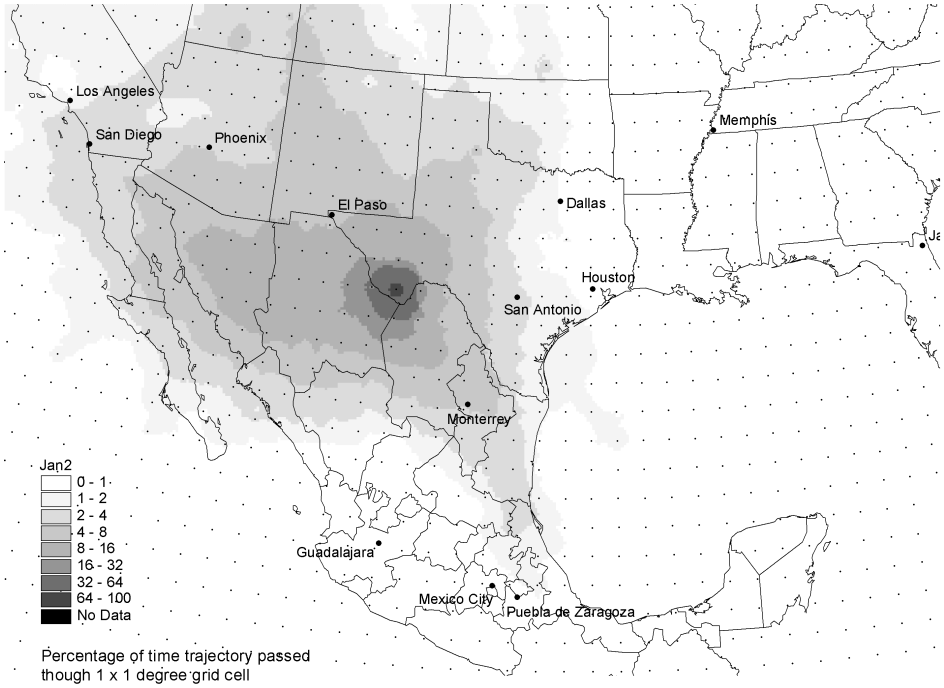

Figure 2- 5 Trajectory frequency for second half of January

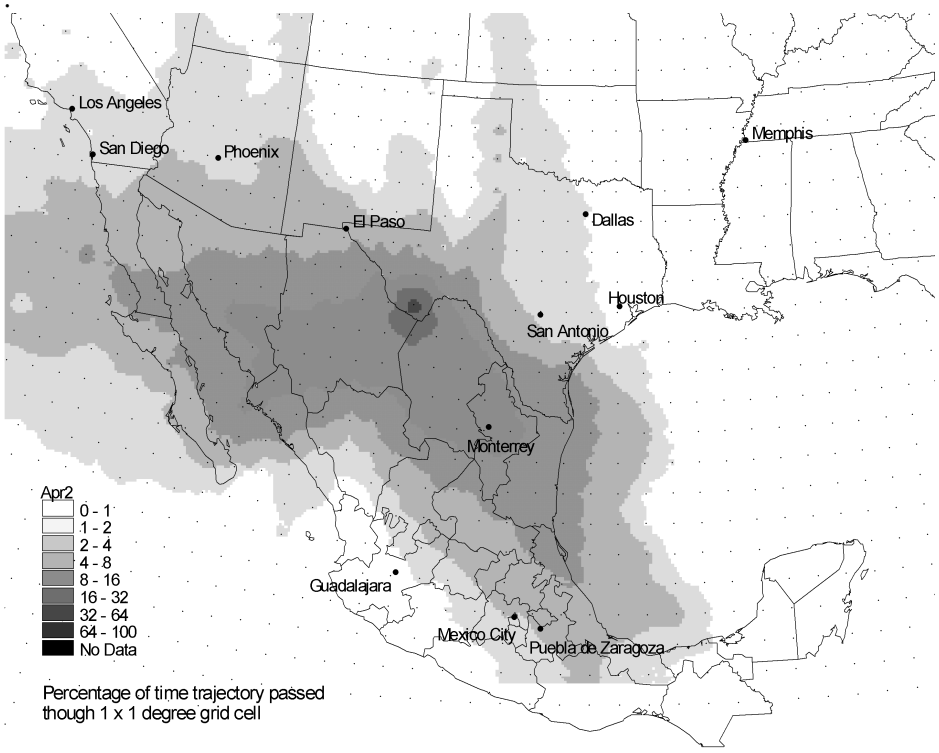

Figure 2- 6 Trajectory frequency for second half of April.

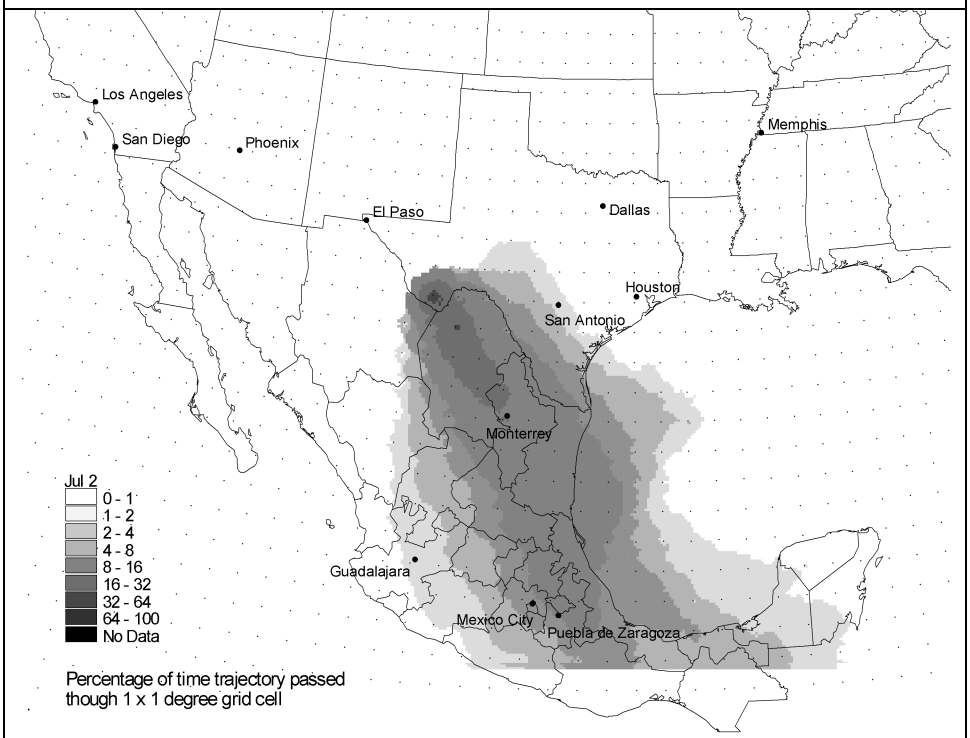

Figure 2- 7 Trajectory frequency for second half of July.

In late summer flows are still dominated by southeasterly backtrajectories, but trajectories from the east or northeast increase, reaching their annual peak frequency (Figure 2-8).

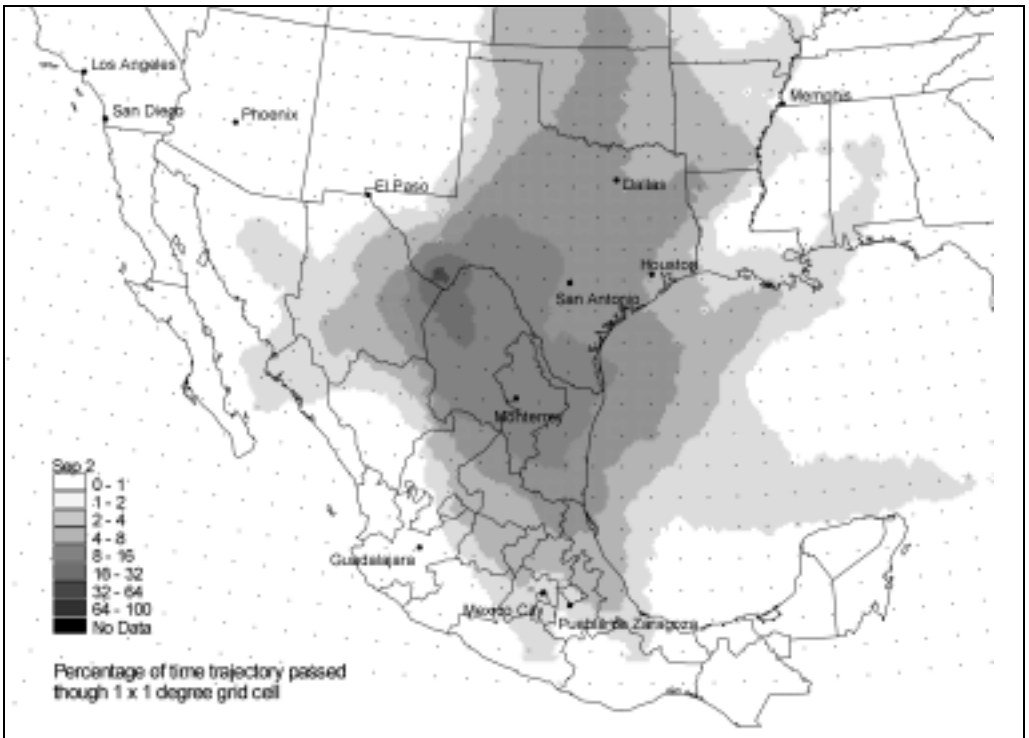

Figure 2- 8 Trajectory frequency for second half of September.

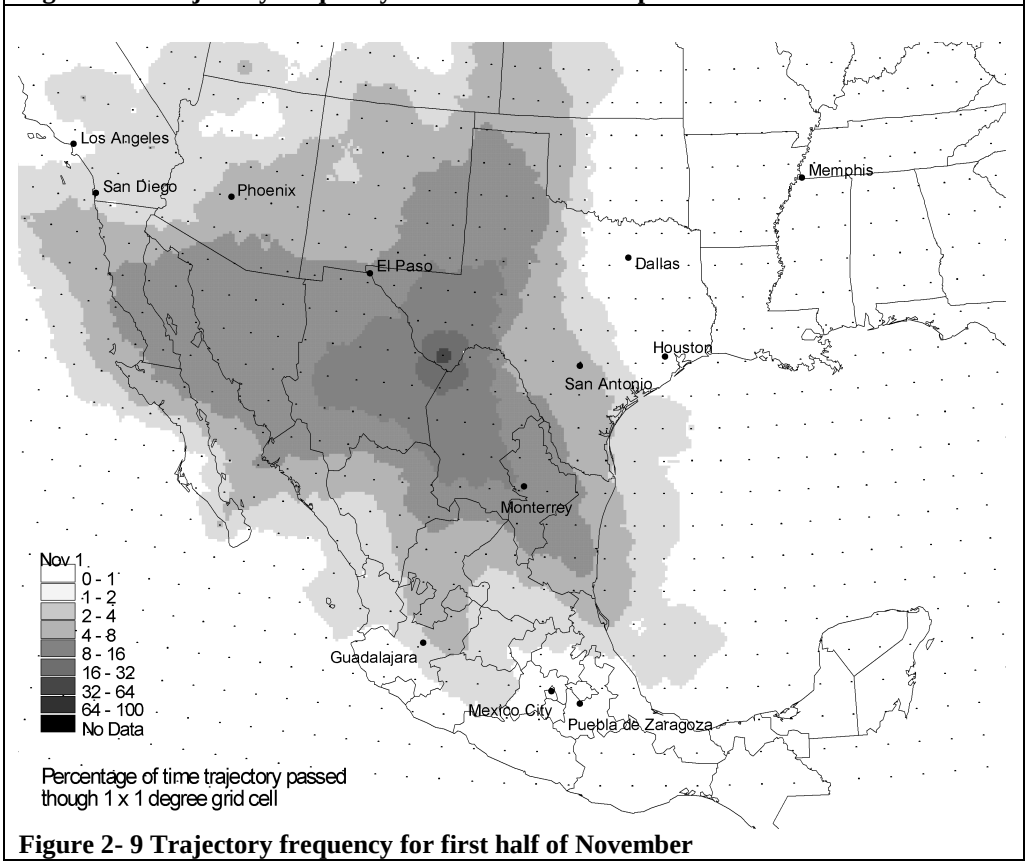

Figure 2- 9 Trajectory frequency for first half of November

By early November, a tri-modal distribution of backtrajectories from the north, west, and southeast is apparent (Figure 2-9). The pattern gradually evolves back to the west & northwest backtrajectories being most frequent in January, completing the annual cycle.

In summary, the backtrajectories in summer are very much dominated by south-easterlies. Easterlies, which are not very common overall, peak during late September. During winter months backtrajectories are mainly from the west and northwest, with few from far to the south. In the transition periods, flow is common from the west, north, and southeast.

Relative effects of transport from some specific source areas

Next we consider relative effects of transport from some specific source areas considering distance from Big Bend and frequency of transport. This assessment was not expected to accurately model the impacts from different source areas; rather it was used for study planning purposes. Figure 2-3 showed estimated SO_2 emissions from 1° latitude by 1° longitude cells. Emissions from sources at a greater distance from BBNP disperse more before reaching BBNP than emissions from more nearby sources. Emissions were weighted by distance (emission rate divided by distance) to account for this effect; the results are shown in Figure 2-10. The inverse distance weighted analysis shows less weighting of the Ohio River Valley sources and much greater weighting for the Carbon I/II powerplants. Other sources in northern and central Mexico and eastern Texas appear to be potentially significant as well. This analysis may give an indication of potential maximum impacts from an area, but does not consider how frequently there is transport and hence total potential impact from the various source areas.

SO_2 emissions were also weighted by the frequency of transport from the source areas to BBNP (Figure 2-11). Due to most frequent transport from the south and southeast and infrequent transport from the northeast, the Mexican sources (especially Carbon I/II, Tula-Vito-Apasco, and the Mexico City area) predominant using this method.

Figure 2-12 shows the frequency of flow by half month period from each selected source area to BBNP using the 12 years of ATAD backtrajectories. These sources included additional regions, such as San Antonio that may not be large SO_2 sources but are sizable area sources of various pollutants that potentially affect visibility. With the exception of locations to the west and north (Cananea , the Texas/New Mexico border, and Ciudad Juarez/El Paso), all of the areas are most frequently transported to BBNP during the period from the beginning of July through the end of October. During the early part of this period emissions from sources in Mexico to the southeast of BBNP are almost exclusively transported to BBNP. At the end of this period, the sources to the northeast (Houston, and the Texas lignite belt power plants) are also transported to BBNP.

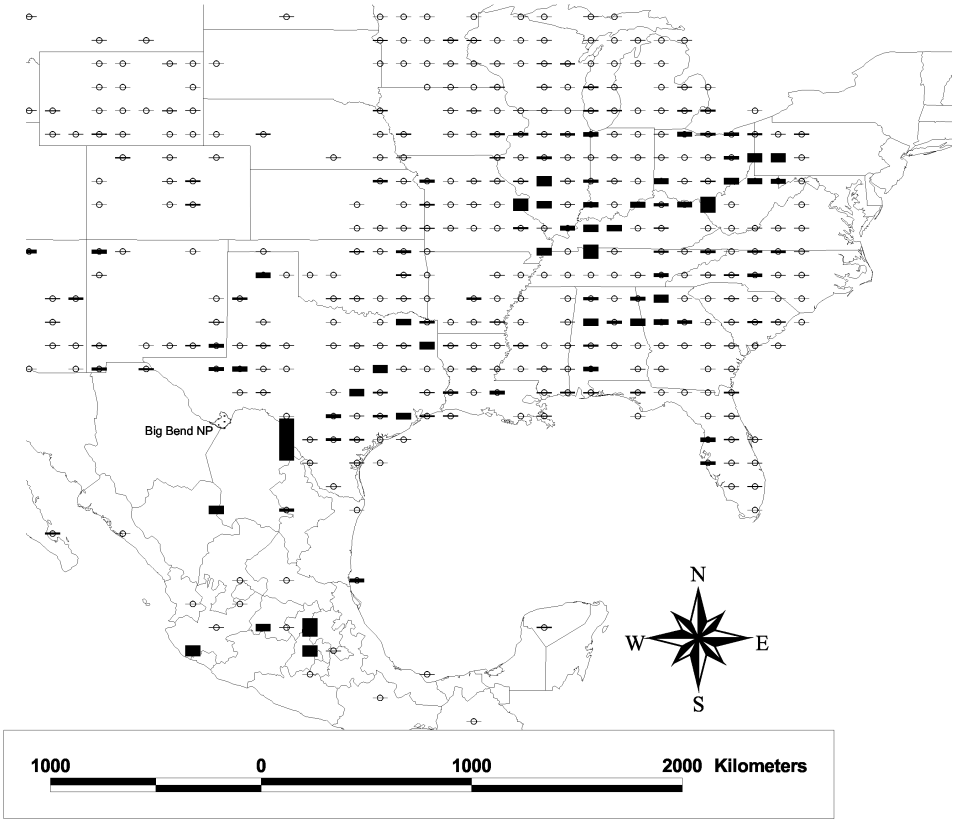

Figure 2-10. Emissions weighted inversely by distance from BBNP for 1° lat. by 1° long. grid cells.

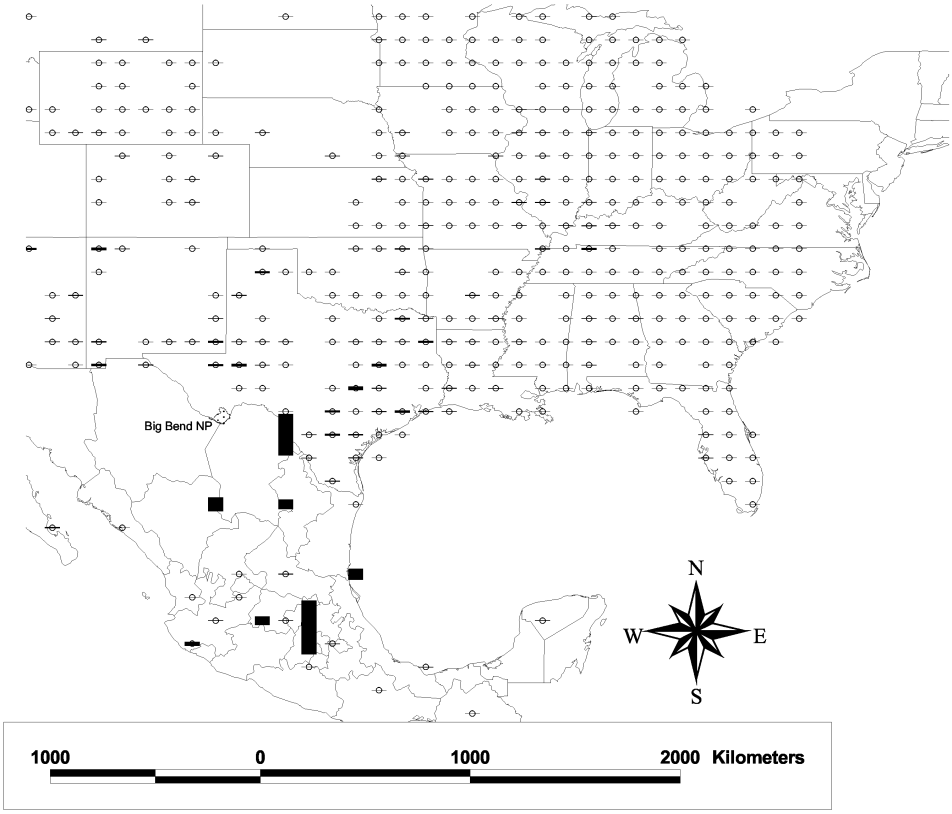

Figure 2-11. Emissions weighted by transport frequency for 1° latitude by 1° longitude grid cells.

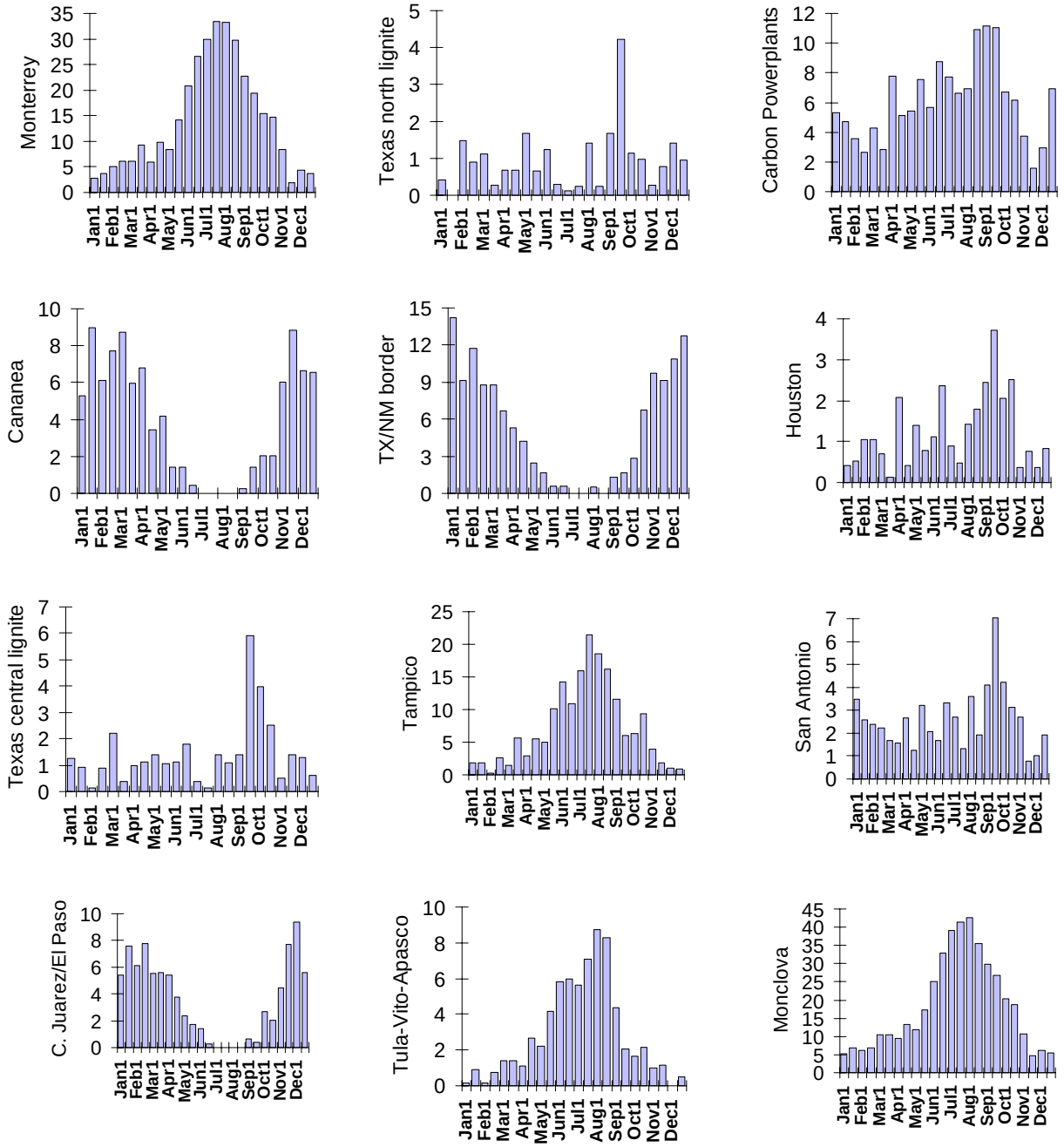

Figure 2-12. Frequency of flow by ½ month periods to Big Bend National Park from selected source areas. Frequency is the percentage of backward trjaectories from Big Bend that passed over the 1 degree latitude by 1 degree longitude cell containing the source area. The relative frequency by time of year is the parameter of interest. The absolute magnitude is an artifact of the grid size (1°x 1°) used.

2.4 Seasonality of light extinction and aerosol components

Figure 2-13 summarizes the tenth, fiftieth, and nintieth percentile levels of light extinction coefficient (b_{ext}) by month, averaged over the period December 1988 – August 1998. Figure 2-14 gives the same information, except that deciview is used in place of light extinction coefficient. Periods with relative humidity greater than 90% are not included. Data flagged for having hourly changes of bext > 10 Mm^{-1}, but not > 90% RH were included (this data represents about 20% of the observations). While there can be substantial variability from year to year, the average pattern shows highest median extinction in May. A rapid increase occurs from March to May (39-56) Mm^{-1}, representing a 60% increase in non-Rayleigh light extinction) and median b_{ext} remains within a few Mm^{-1} from May through September, after which extinction decreases. This pattern is similar for the tenth and ninetieth percentiles of extinction. At the 90th percentile, a relative minimum occurs in July. In summary, light extinction levels are lowest in winter (November-March), and highest in summer (May-September), with transition periods in the spring and fall. May 1998 had particularly high light extinction due to large fires in Mexico (Yucatan Peninsula, especially).

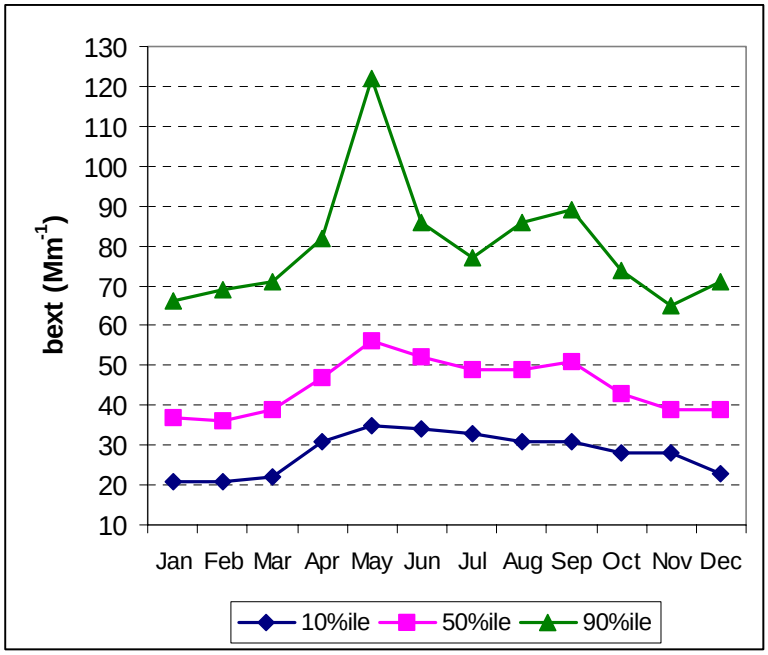

Figure 2-13. 10, 50, and 90 percentile b_{ext} values at Big Bend National Park (Dec 1988—August 1998). Data with relative humidity greater than 90% are not included.

Sisler, *et al.* (1996) used IMPROVE aerosol data to estimate the percent of aerosol light extinction from each of the major components for the period March 1992-February 1995. Their results (Table 2-1) show that sulfate is the most important contributor to light extinction at Big Bend, and organic compounds, light absorbing compounds, and crustal material are also important.

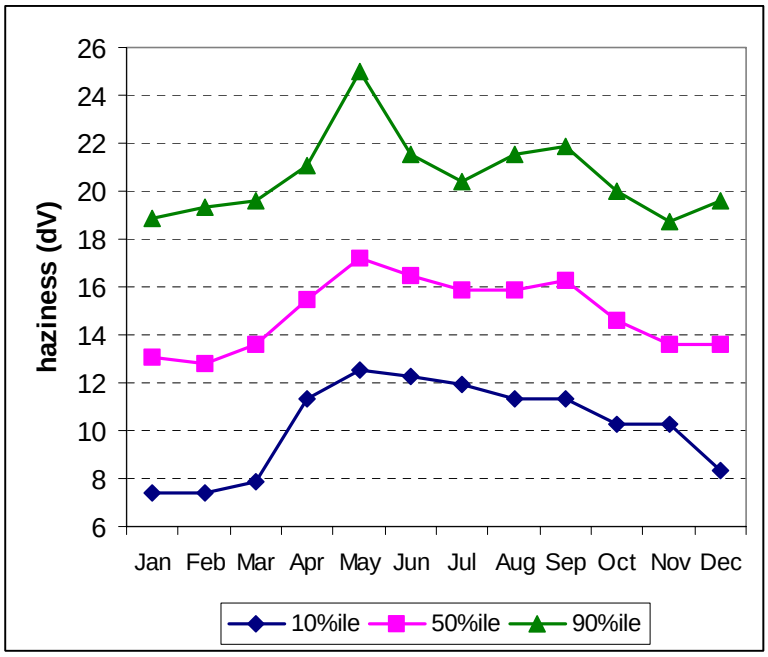

Figure 2-14. 10, 50, and 90 percentile haziness in deciview at Big Bend National Park (December 1988—August 1998). Data with relative humidity greater than 90% are not included.

Table 2-1
Average percent of reconstructed aerosol light extinction by component

Component	Percent of aerosol light extinction
Sulfate	41
Nitrate	3.8
Organics	19
Light absorption	21
Crustal	16

Table 2-1 shows that sulfate is the most important contributor to light extinction at Big Bend, and organics, light absorbing compounds, and crustal material are also important.

Variability in monthly averaged aerosol component concentrations for the period March 1988- February 1999 are shown in Figure 2-15. Elemental carbon (EC), organic carbon (OC) and fine mass all peak in May. This is the same month as the peak in b_{ext}. A few very high values of EC and OC in May suggest that fires (agricultural and wildfires) may be particularly important during this time of year (especially for May 1998).

Average monthly particulate sulfur is similarly high for May through October, except for a dip in concentrations in July. Fine soil is lowest in winter and shows a pronounced peak in July. The July peak is expected to result from transport of Saharan dust. Perry, et. al, (1997) demonstrated transport of Saharan dust into the southern and eastern United States, including Big Bend National Park. The Saharan dust is characterized by a deficit of calcium, leading to higher ratio of aluminum to calcium and silicon to calcium for periods with significant concentrations of Saharan dust present. Table 2-2 shows the monthly averaged silicon divided by monthly averaged calcium at Big Bend. For most months, the ratio is between 2 and 3; for July it is over 6 (also elevated in August). This suggests that Saharan dust is responsible for the peak in fine soil in July. Table 2-2 also shows monthly average fine soil divided by monthly averaged coarse mass. This increase in July and the fact that coarse mass (often associated with soil) does not show a peak in July (Figure 2-15) is consistent with the expectation that a significant fraction of the fine soil in July is transported from Africa.

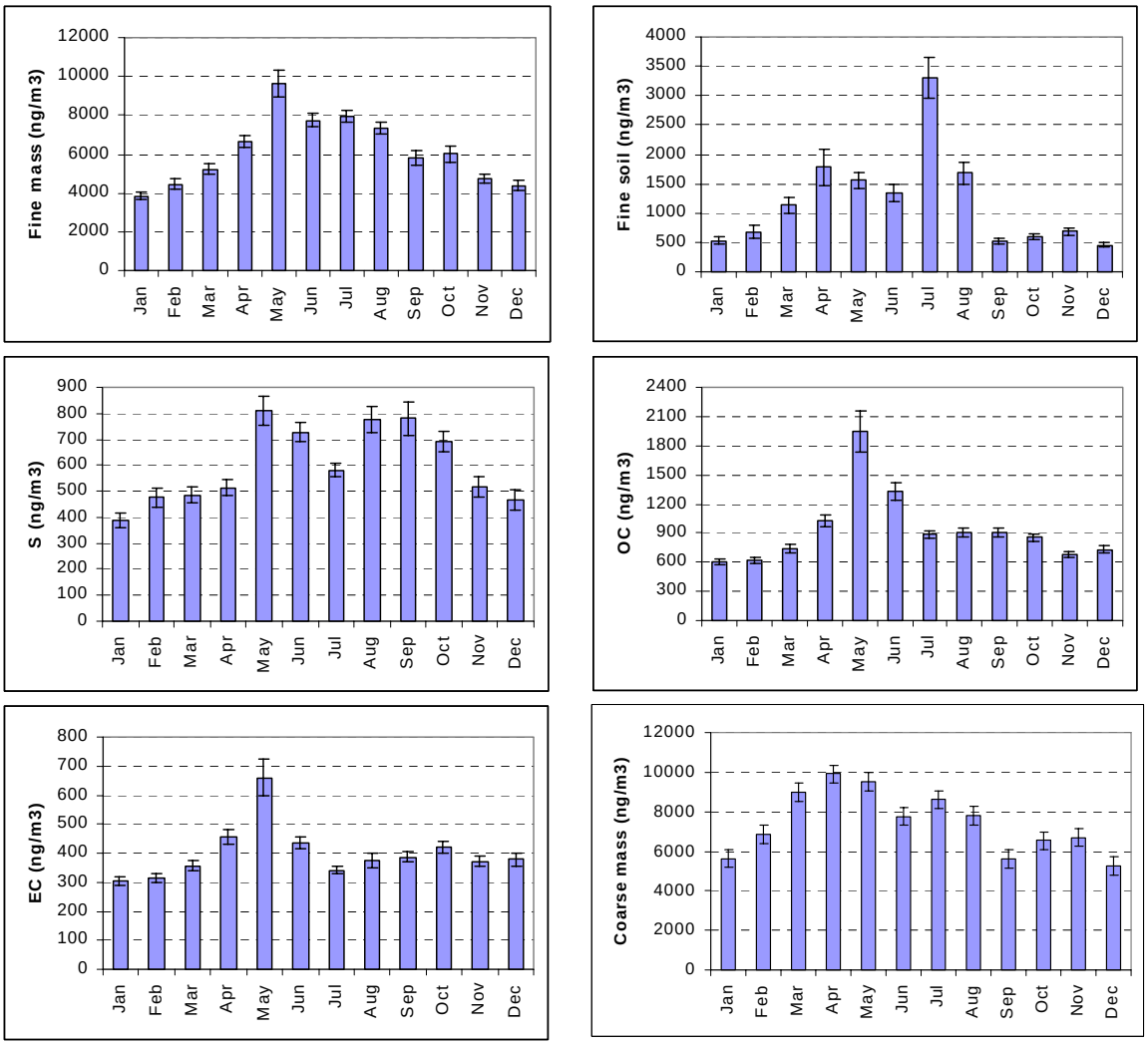

Figure 2-15. Monthly averaged concentration of aerosol components. Error bars show the standard error of the mean. Time period is from March 1988 – February 1999.

Table 2-2. Monthly averaged silicon divided by monthly average calcium and monthly average fine soil/ monthly average coarse mass: December 1988- February 1999.

	Jan	Feb	Mar	Apr	May	Jun	Jul	Aug	Sep	Oct	Nov	Dec
Si/Ca	2.36	2.70	3.02	3.14	2.76	3.18	6.22	5.06	2.93	2.08	2.32	2.12
fine soil/CM	0.09	0.10	0.13	0.18	0.16	0.17	0.38	0.22	0.09	0.09	0.10	0.09

2.5 Relationship between light extinction, chemical components, and backtrajectories

The analyses presented here relate backtrajectories from Big Bend passing through each grid cell to b_{ext} and chemical components measured at Big Bend for the period December 1988- December 1994. These are presented in the form of conditional probability maps which give the probability that a condition is met for the backtrajectories passing through each grid cell. For light extinction coefficient (b_{ext}), particulate sulfur, organics, fine soil, organic carbon, and elemental carbon, the condition was that high (80 percentile or higher) concentrations occurred. It should be noted that these maps show the probability that high concentrations occurred when backtrajectories passed over an area; **they do not reflect average impacts of an area because some areas have much more frequent transport to Big Bend than other areas, as shown earlier.** It should also be noted that grid cells associated with a high frequency of certain conditions, such as high particulate sulfur at Big Bend should not be assumed to be contributing substantially to these conditions; rather, there are most likely sources somewhere along the trajectories passing over these cells that are contributing to the high concentrations.

Light extinction (b_{ext})

Figure 2-16 shows the frequency of backtrajectories passing through each grid cell for which b_{ext} at Big Bend was at the 80 percentile (57 Mm^{-1}) or higher. Figure 2-16 shows that areas to the northeast through south are relatively likely to be associated with high extinction when the air passes over these areas. Areas from the southwest through north are relatively less likely to be associated with high b_{ext} when the air passes over these areas.

Particulate sulfur

Figure 2-17 shows the conditional probability for high particulate sulfur concentrations (80 percentile = 929 ng/m^3). High sulfur concentrations are relatively likely for backtrajectories from areas northeast through south of Big Bend, with high concentrations unlikely to be associated with backtrajectories from the west-southwest through the north. Although they were not frequent, backtrajectories passing over east Texas and Louisiana were the most likely to be associated with high sulfur at Big Bend.

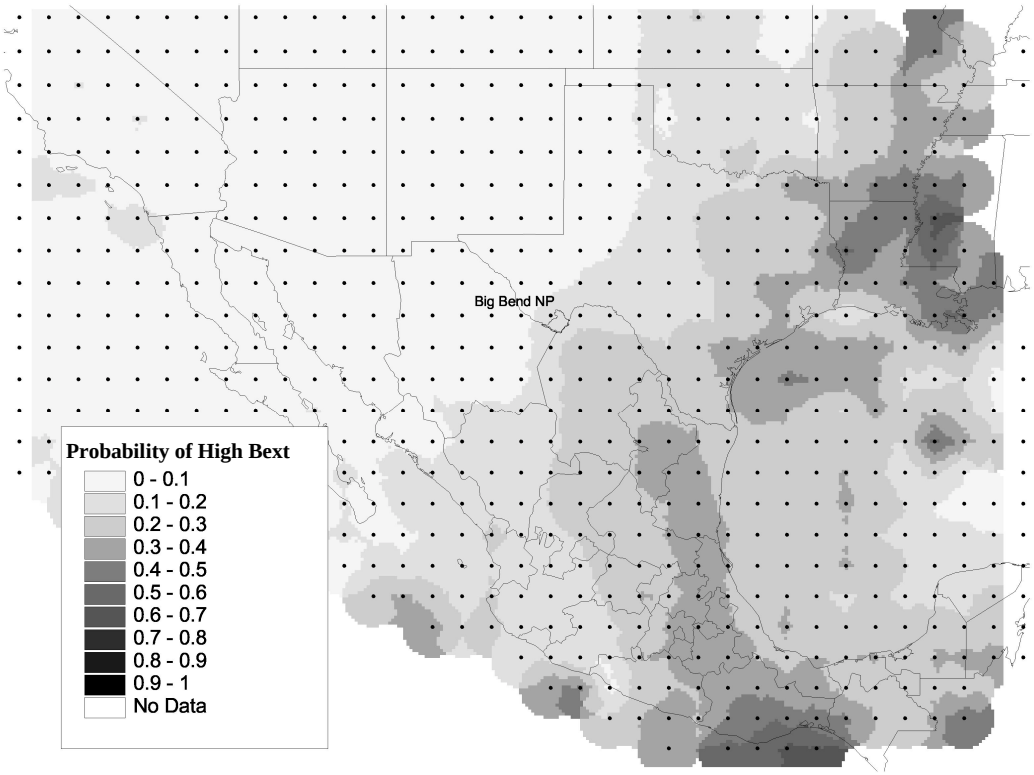

Figure 2-16: Probability that a trajectory passing over a cell will be associated with a b_{ext} value at BBNP above the 80 percentile value (57 Mm^{-1}).

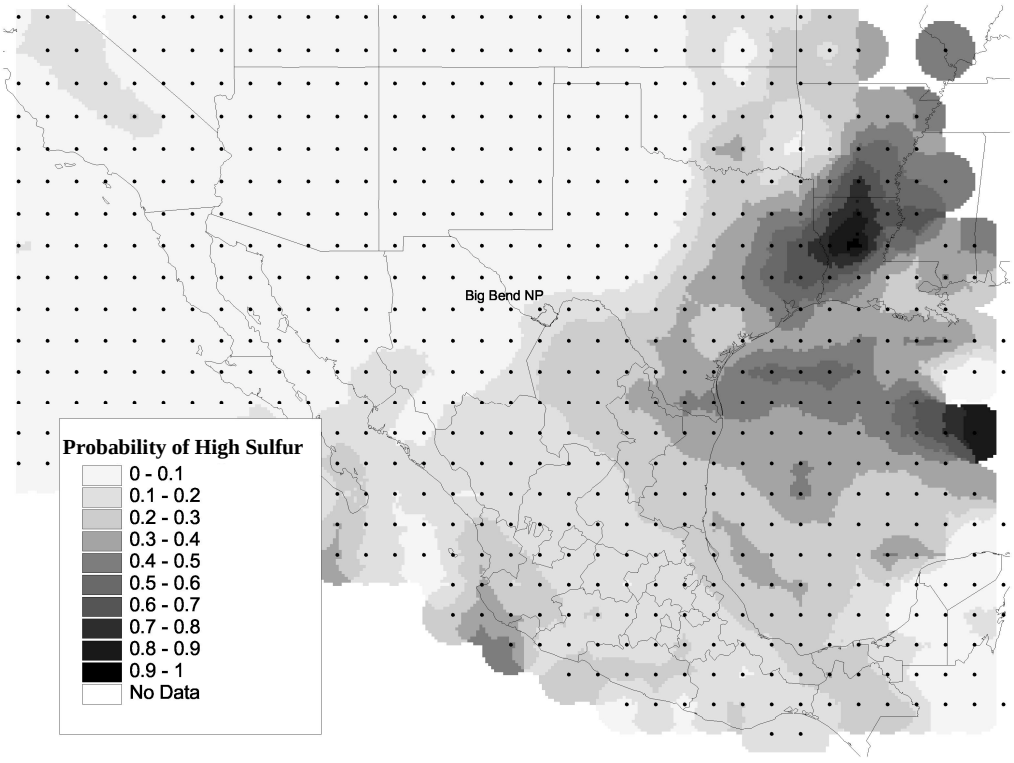

Figure 2-17: Probability that a trajectory passing over a cell will be associated with a particulate sulfur concentration at BBNP above the 80 percentile value (929 ng/m^3).

Light absorption (b_{abs})

Figure 2-18 shows that high levels of b_{abs} (80 percentile = 10.0 Mm^{-1}) are most likely for backtrajectories from the northeast clockwise through the west-southwest. The highest probability is associated with backtrajectories passing through east Texas and Louisiana.

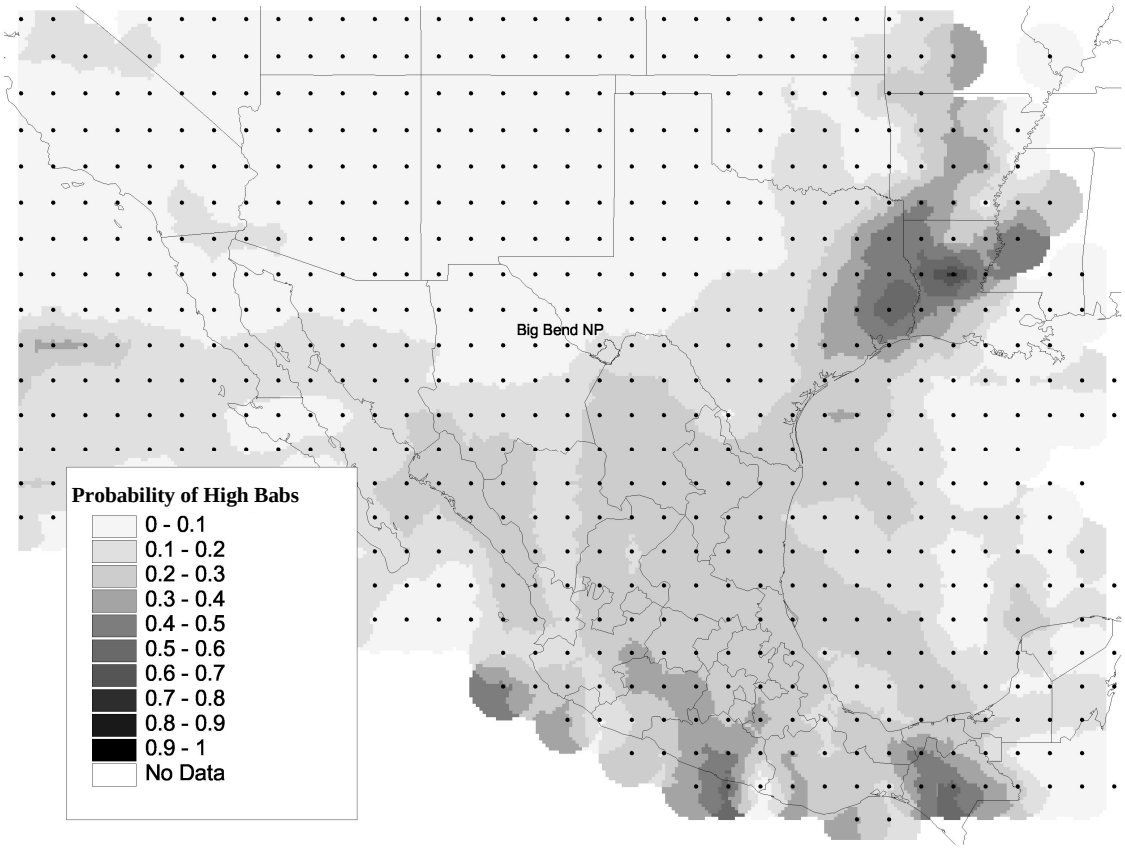

Figure 2-18: Probability that a trajectory passing over a cell will be associated with a b_{abs} value at BBNP above the 80 percentile value (9.96 Mm-1).

Elemental Carbon

Conditional probability for high elemental carbon (80 percentile = 555 ng/m3) is shown in Figure 2-19. Backtrajectories from the north-northeast clockwise through the west are relatively likely to be associated with high elemental carbon at Big Bend, especially backtrajectories passing over east Texas. Another area off the northern California coast is indicated to be associated with high elemental carbon; due to the small number of backtrajectories from this area, this result may not be meaningful.

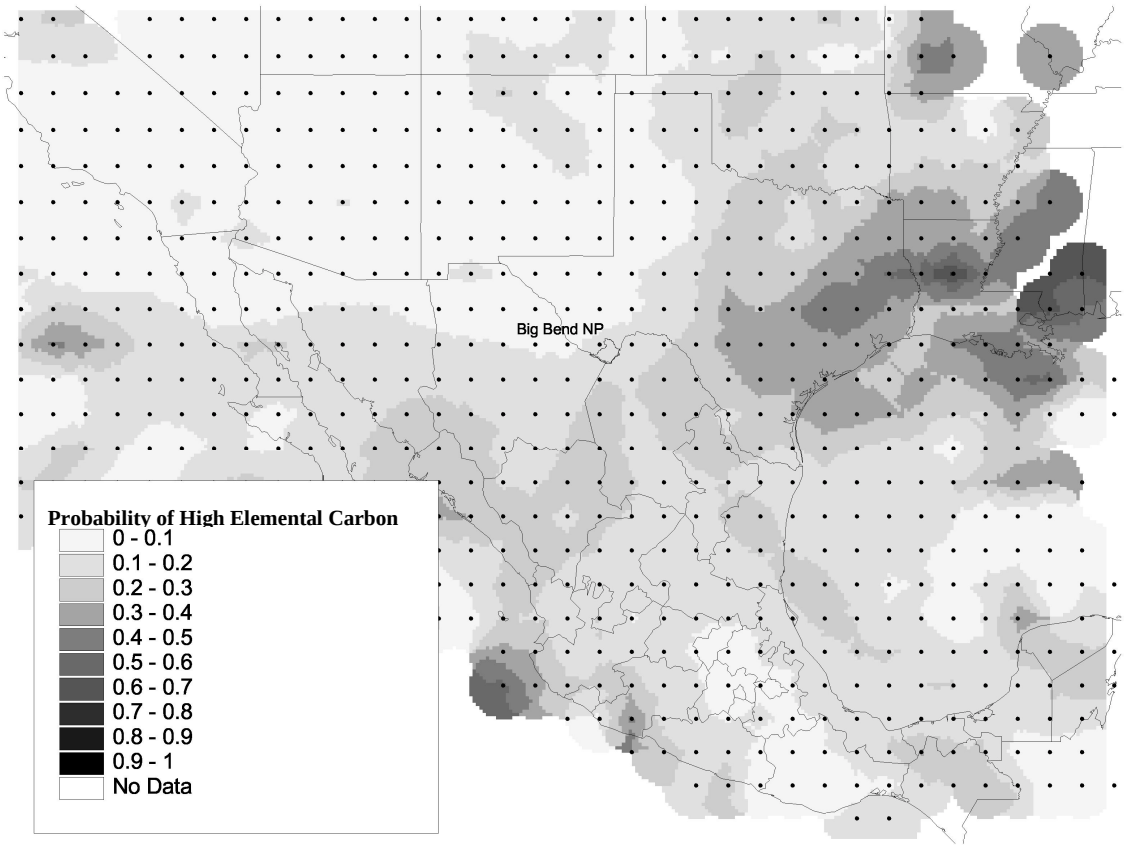

Figure 2-19: Probability that a trajectory passing over a cell will be associated with an elemental carbon concentration at BBNP above the 80 percentile value (555 ng/m^3).

Organic Carbon

High concentrations of organic carbon (80 percentile = 1208 ng/m^3) are most likely for backtrajectories passing over the coastal or near- coastal Gulf of Mexico in Mexico, Texas and Louisiana (Figure 2-20). High organic carbon concentrations are unlikely for backtrajectories from the northwest.

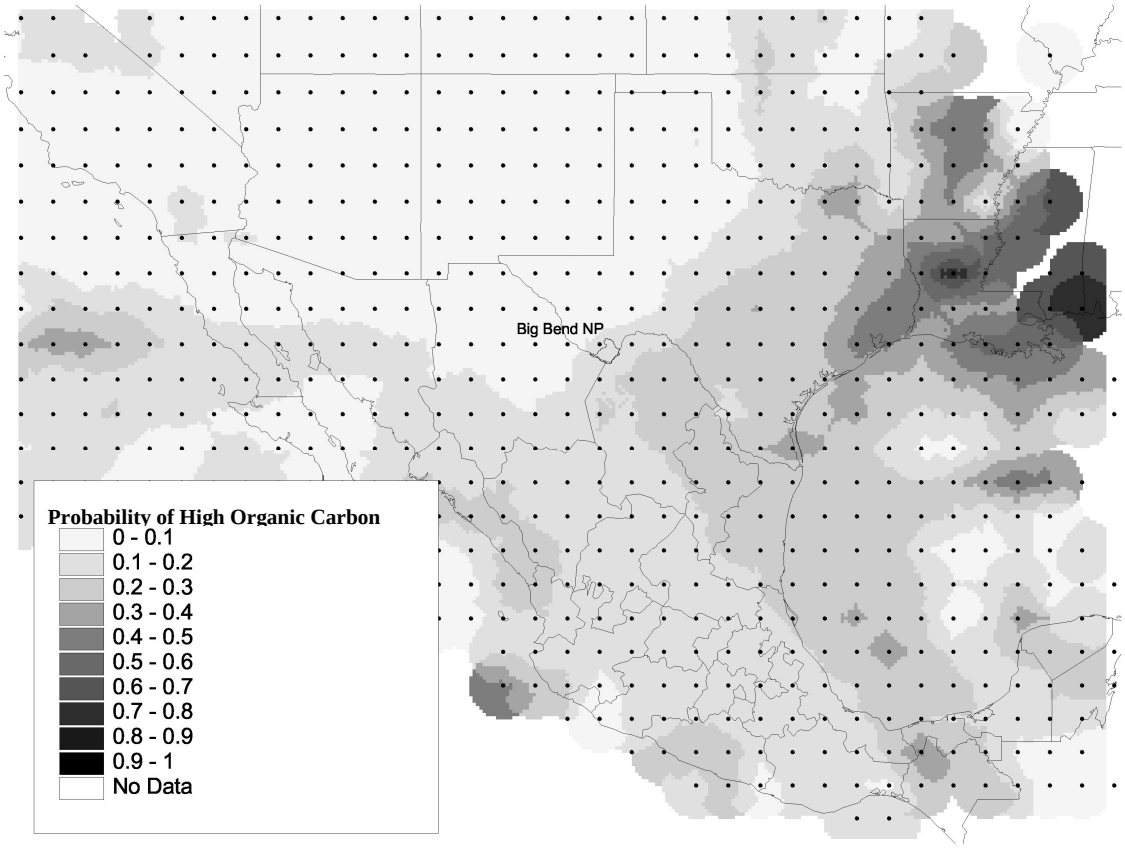

Figure 2-20: Probability that a trajectory passing over a cell will be associated with an organic carbon concentration at BBNP above the 80 percentile value (1208 ng/m^3).

Fine soil

Figure 2-21 shows the conditional probability for high concentrations of fine soil (80 percentile = 1690 ng/m^3). High fine soil is associated with backtrajectories from two areas: 1) southeast of Big Bend National Park and 2) long distances to the northwest. The areas far to the northwest are not likely the actual source of the fine soil; rather for backtrajectories to reach Big Bend during the 5-day backtrajectory, high wind speeds are required. Thus, flow from these distant regions is probably associated with high wind speeds, which would suspend soil materials from disturbed areas anywhere along the backtrajectory. We do see high fine soil associated with backtrajectories to the southeast over Mexico. The greater probability of high fine soil for distant backtrajectories from the southeast might be explained in terms of higher wind speeds, as discussed above. However, backtrajectories from the east may also include transport of Saharan dust into the area, as described above.

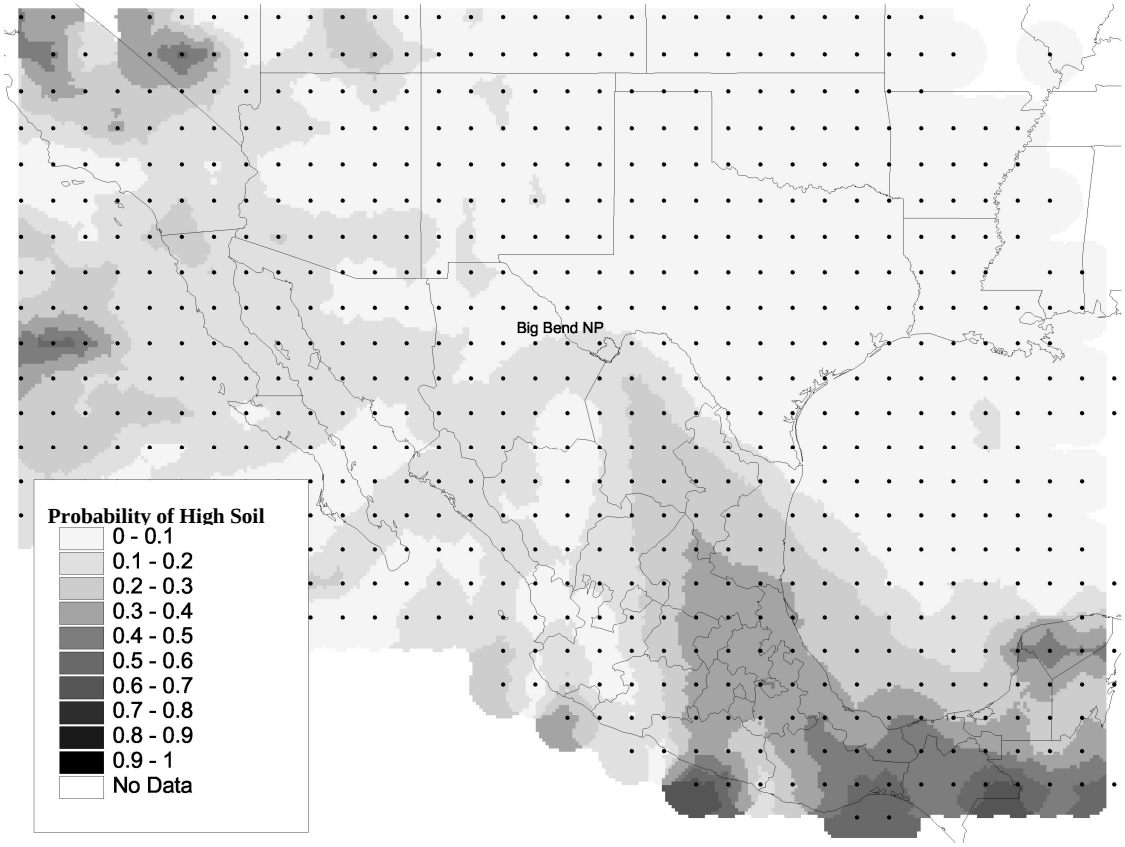

Figure 2-21: Probability that a trajectory passing over a cell will be associated with a fine soil concentration at BBNP above the 80 percentile value (1690 ng/m^3).

Relative Humidity

Because high humidity is required for water growth of hygroscopic aerosols, such as ammonium sulfate, and high humidity is often accompanied by clouds that enable rapid conversion of SO_2 to sulfate, it is informative to examine backtrajectory and relative humidity relationships. Figure 2-22 is a conditional probability that backtrajectories that passed through grid cells coincided with high (>70%) relative humidity at Big Bend. Overall, 19% of the backtrajectories from Big Bend met this criterion. The plot shows a clear division between backtrajectories with an easterly component which were likely to be associated with high relative humidity, and backtrajectories with a westerly component, which were unlikely to be associated with high relative humidity. Backtrajectories passing through the Gulf of Mexico to the east to southeast of Big Bend were especially likely to be associated with high RH at Big Bend. These areas have their peak transport toward Big Bend in September, which also has the highest average rainfall of any month along the south Texas coast. Thus, while the high RH and clouds associated with these backtrajectories will likely allow for high conversion and water growth of hygroscopic particles, offsetting effects of washout of particles may occur.

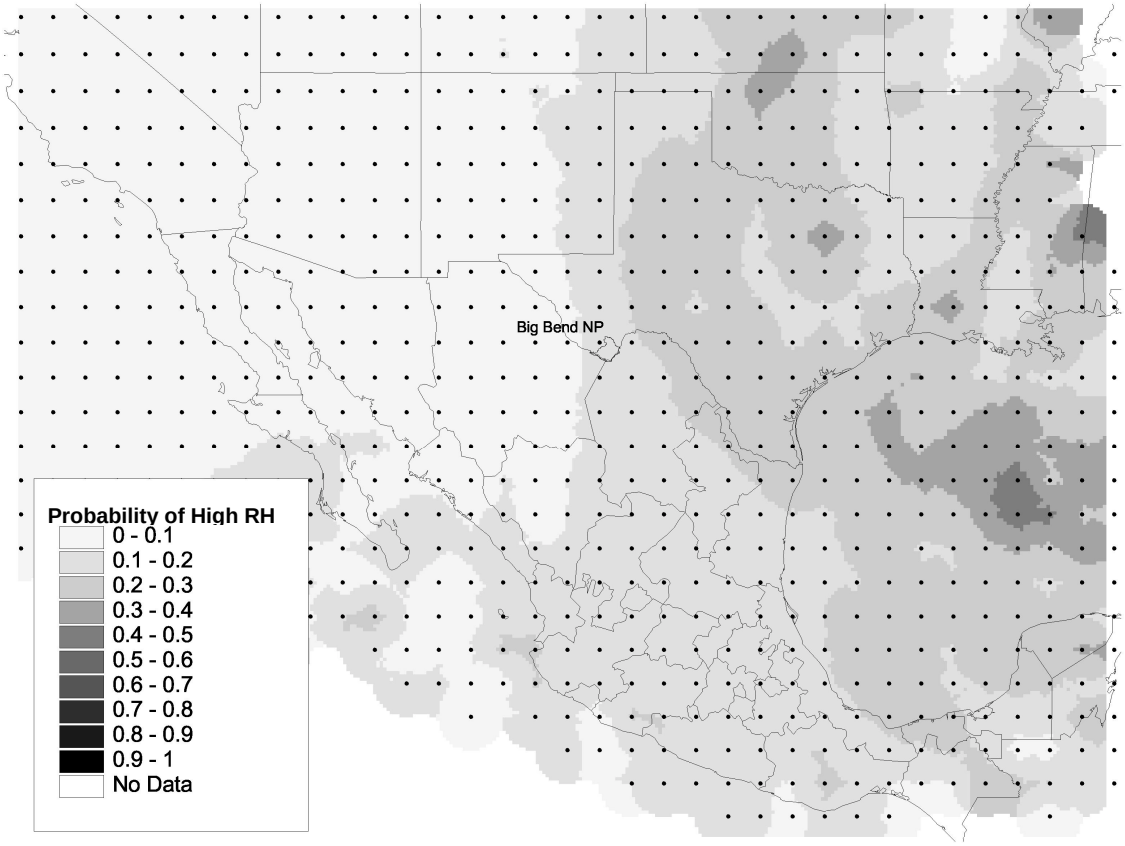

Figure 2-22: Probability that a trajectory passing over a cell will be associated with a relative humidity at BBNP above the 80 percentile value (70% RH).

2.6 Study Design Considerations

The material presented earlier in this section regarding monthly-summarized visibility and aerosol composition at Big Bend, transport patterns during periods of poor visibility, the spatial distribution of SO_2 emissions, and the frequency these emissions are transported toward Big Bend helped guide the BRAVO study design. Also helping to guide the BRAVO design was knowledge gained from previous studies, notably the preliminary Big Bend study and Project MOHAVE.

Particulate sulfate has been the compound that contributes most to visibility impairment at Big Bend National Park; thus sources of SO_2 are of particulate interest to BRAVO. Particulate carbon (elemental and organic) also contributes substantially to haze at Big Bend; the aerosol monitoring program (section 4.1) was designed to reveal more information regarding sources of carbonaceous aerosol at Big Bend.

On the average, visibility at Big Bend is most impaired during the May to September period. However, in October transport from the northeast is sometimes associated with very poor visibility. A four-month field program from July through October 1999 was selected to maximize the number of occurrences of flow from two regions of particular interest: northeast Mexico and eastern Texas. Backtrajectory analysis showed that this four month period would maximize the number of occurrences of flow from the significant source areas for SO_2 that are closest to Big Bend National Park. These periods would also be expected to give many episodes of transport from large SO_2 sources in central Mexico and would likely result in one or more cases of transport from large SO_2 source regions in the Ohio River Valley.

The use of tracers in Project MOHAVE showed that the current state of atmospheric transport and dispersion modeling in complex terrain is not sufficiently correct to draw reliable conclusions regarding source-receptor relationships on a day-by-day basis (Pitchford *et. al.*, 1999, Green and Tombach, 2000). This result argued for the release of artificial tracers for use in direct attribution methods such as TAGIT (Kuhns et al. 1999), to help evaluate and calibrate transport and dispersion models, and for use in receptor based models. The tracer program design is considered in more detail in section 3.

Previous studies also demonstrated the utility of a large network of particulate monitoring sites and chemical analysis of the filter samples. As discussed further in section 5, several analysis methods utilize this spatially resolved aerosol data. BRAVO design included a network of 37 aerosol monitoring sites. Purposes of the individual monitoring sites for BRAVO are described in section 4.1 (Table 4-2). Additional aerosol studies were conducted (mainly at Big Bend) to answer questions remaining after the preliminary study.

Additional upper air measurements were made to help evaluate and calibrate wind field models for input to air quality models (section 4.3). Extensive optical measurements at Big Bend National Park (section 4.2) were made to help characterize

effects of relative humidity on light scattering and the relative effects of fine and coarse particles on light scattering and light absorption. To help separate the effects from different sources, a source characterization program (sampling and chemical analysis of emissions) was conducted for several source types (section 4.4).

Unfortunately, the study design was constrained by the inability of the United States and Mexico to agree on the design for a joint U.S.- Mexico study. This resulted in a study design that included monitoring and source characterization only in the United States. Earlier versions of the proposed study plan included substantial aerosol and source monitoring and tracer release in Mexico. The final plan includes additional monitoring and tracer release along the U.S.- Mexico border to partly alleviate the limitations imposed from conducting a U.S. only study.

3 Tracer Release

3.1 Tracer Study Objectives

The objectives of the tracer study are to:

1) Tag (track emissions transport from) large individual sources with the potential for significant visibility impairment at Big Bend National Park
2) Tag source areas with the potential for significant visibility impairment at Big Bend National Park
3) Evaluate and improve performance of air quality models used for BRAVO.

For objective 1, tagging large individual point sources can be used in direct attribution analysis methods, such as TAGIT (Kuhns, et. al. 1998), which looks for gradients in particulate sulfur between source affected areas and areas outside the influence of emissions from the tagged source. The tracer can also be used to determine periods when the tagged source did not affect Big Bend National Park.

In objective 2, the tracer is used to give the general transport pattern and dispersion for emissions from a given source area. Because tracer is released from a point within an area of multiple sources, direct source attribution is not possible. The results are a qualitative demonstration of transport from the source region as well as information useful for objective 3. It identifies periods in which a source area is likely contributing to visibility impairment, but does not give a direct estimate of the impairment attributable to the source area.

Meeting objective 3 is useful for modeling the effects of tagged and non-tagged sources alike. This includes obtaining transport and dispersion, against which model results can be evaluated. Ideally, transport time would also be given. Model performance may be improved by adjusting dispersion parameters, etc. within a reasonable range that provides for improved model performance. As discussed in the following section, the tracer study is subject to constraints that affect the study design.